

# Lifting the Bandwidth Limit of Optical Homodyne Measurement

Yaakov Shaked, Yoad Michael, Rafi Z. Vered, Leon Bello, Michael Rosenbluh and Avi Pe'er<sup>1</sup>

<sup>1</sup>*Department of Physics and BINA Center of Nano-technology,  
Bar-Ilan University, Ramat-Gan 52900, Israel\**

## Abstract

Homodyne measurement is a corner-stone of quantum optics [1]. It measures the fundamental variables of quantum electrodynamics - the quadratures of light, which represent the cosine-wave and sine-wave components of an optical field. The quadratures constitute the quantum optical analog of position and momentum in mechanics and obey quantum uncertainty, indicating the inherent inability to measure both simultaneously [2]. The homodyne process, which extracts a chosen quadrature amplitude by correlating the optical field against an external quadrature reference (local-oscillator, LO), forms the backbone of coherent detection in physics and engineering, and plays a central role in quantum information processing. Homodyne can reveal non-classical phenomena, such as squeezing of the quadrature uncertainty [3]; It is used in tomography to fully characterize quantum states of light [4, 5]; Homodyne detection can generate non-classical states [6], provide local measurements for teleportation [7–9] and serve as a major detector for quantum key distribution (QKD) and quantum computing [10, 11]. Yet, standard homodyne suffers from a severe bandwidth limitation. While the bandwidth of optical states can easily span many THz, standard homodyne detection is inherently limited to the electrically accessible, MHz to GHz range [12–15], leaving a dramatic gap between the relevant optical phenomena and the measurement capability. This gap impedes effective utilization of the huge bandwidth resource of optical states [11, 16] and the potential enhancement of the information throughput *by several orders of magnitude* with parallel processing in quantum computation, QKD and other applications of quantum squeezed light. Here we demonstrate a fully parallel optical homodyne measurement across an arbitrary optical bandwidth, effectively lifting the bandwidth limitation completely. Using optical parametric amplification, which amplifies one quadrature while attenuating the other, we measure two-mode quadrature squeezing of 1.5dB below the vacuum level simultaneously across a bandwidth of 55THz using a single LO - the pump. This broadband parametric homodyne measurement opens a wide window for parallel processing of quantum information [11, 17–19].

It is standard practice to express the field of nearly monochromatic light  $E(t) = |A| \cos(\Omega_0 t + \varphi)$ , as a superposition of two quadrature oscillations:  $E(t) = X \cos \Omega_0 t + Y \sin \Omega_0 t$ , where  $X$  and  $Y$  are the real quadrature amplitudes. While this separation is just a mathematical convenience in classical electromagnetism, it is of fundamental importance in quantum optics, since the quadratures are a conjugate pair of non-commuting observables ( $[X, Y] = 2i$ ) that obeys quantum uncertainty ( $\Delta X \Delta Y \geq 1$ ), just like position and momentum. This conjugation is most emphasized with squeezed light, where the uncertainty of one quadrature of the field is reduced (squeezed), while the uncertainty of the other is inevitably increased (stretched)  $\Delta X < 1 < \Delta Y$ .

Although formally, generalization of the quadrature description to a broadband time-dependent field using time-dependent quadratures  $x(t), y(t)$  is direct, the homodyne method for measuring the quadratures inherently distinguishes between a nearly monochromatic field and a broadband field. What distinguishes between the two cases is the MHz to GHz electronic bandwidth of standard homodyne detection. In the near monochromatic case, the instantaneous quadrature amplitudes vary slowly over millions of optical cycles, and can be directly observed through the time dependent electrical signal of the homodyne photo-detectors. However, in the case of broadband light, the response of the photo-detectors is too slow to follow the rapid variations of the quadrature amplitudes, which can easily be at optical frequencies. Broadband signals require therefore an inherently different measuring technique.

The direct mathematical relation between the broadband quadrature amplitudes and the field is simple and illuminating in both time and frequency, and yet, it is rarely used outside the context of near monochromatic light. Defining the field as  $E(t) = A(t) \exp i\Omega_0 t + c.c.$  ( $A(t)$  the complex field amplitude), the two quadratures in time are simply the real and imaginary parts of  $A(t)$

$$\begin{aligned} x(t) &= A(t) + A^*(t) = 2\text{Re}A(t), \\ y(t) &= i[A^*(t) - A(t)] = 2\text{Im}A(t). \end{aligned} \tag{1}$$

In frequency, the quadrature amplitudes  $x(\omega), y(\omega)$  are complex in general and represent the symmetric and antisymmetric parts of the field spectral amplitude  $A(\omega)$

$$\begin{aligned} x(\omega) &= A(\omega) + A^*(-\omega), \\ y(\omega) &= i[A^*(\omega) - A(-\omega)], \end{aligned} \tag{2}$$

where  $\omega$  is the offset frequency from the carrier  $\Omega_0$ . Thus, the fundamental quadrature

oscillation - a single frequency component of the quadrature amplitudes  $x(\omega), y(\omega)$ , is a two-mode combination of frequencies  $\omega_s = \Omega_0 + \omega$  and  $\omega_i = \Omega_0 - \omega$ , commonly termed signal and idler. In time, this quadrature oscillation represents a two-mode beat envelope at frequency  $\omega$  on a pure cosine (sine) carrier-wave of frequency  $\Omega_0$ , where the envelope amplitude is  $|x(\omega)|(|y(\omega)|)$  and phase  $\varphi_{x,(y)}(\omega)$

$$\begin{aligned} x_\omega(t) &= |x(\omega)| \cos(\omega t + \varphi_x) \cos \Omega_0 t \\ &= [\text{Re}x(\omega) \cos \omega t + \text{Im}x(\omega) \sin \omega t] \cos \Omega_0 t. \end{aligned} \quad (3)$$

In analogy to eq. 2, the quantum operators for the spectral quadratures  $x(\omega), y(\omega)$  can be expressed in terms of the signal and idler field operators  $a_s, a_i$  [20]

$$\begin{aligned} x(\omega) &= a_s + a_i^\dagger \\ y(\omega) &= i [a_s^\dagger - a_i], \end{aligned} \quad (4)$$

which preserve the commutation relation  $[x, y] = 2i$  and reduce in the monochromatic case to the single-mode quadratures  $X = a + a^\dagger, Y = i(a^\dagger - a)$ . Although these two-mode quadratures are non-hermitian, they are still observable quantities, since  $x$  commutes with its conjugate ( $[x, x^\dagger] = 0$ , as opposed to  $[a, a^\dagger] = 1$ ), allowing simultaneous measurement of both the real and imaginary part of the quadrature (or amplitude and phase).

$$\begin{aligned} \text{Re}x &= x + x^\dagger = X_s + X_i \\ \text{Im}x &= i(x - x^\dagger) = Y_s - Y_i, \end{aligned} \quad (5)$$

where  $X_{s,i}, Y_{s,i}$  are the standard single mode quadratures of the signal and idler modes.

To measure the field quadratures, the optical signal should be compared against a strong and coherent quadrature reference (local oscillator - LO), where the specific quadrature to be measured is dictated by tuning the LO phase. Hence, at the heart of a homodyne detector are an external LO and a field multiplier. In the radio-frequency (RF) domain, for instance, the input radio-wave is directly multiplied with the LO using an RF frequency mixer. In optics, however, direct frequency mixers do not exist and standard optical homodyne relies on a beam splitter to superpose the optical input and the LO (see inset of figure 1) and on the *nonlinear electrical response* of square-law photo-detectors to multiply the two fields and generate an *electronic signal* proportional to the measured  $X$  ( $Y$ ) quadrature. However, the use of square-law photo-detectors as a homodyne multiplier inherently limits the observable time variations of the quadratures to the electronically accessible photo-detector bandwidth

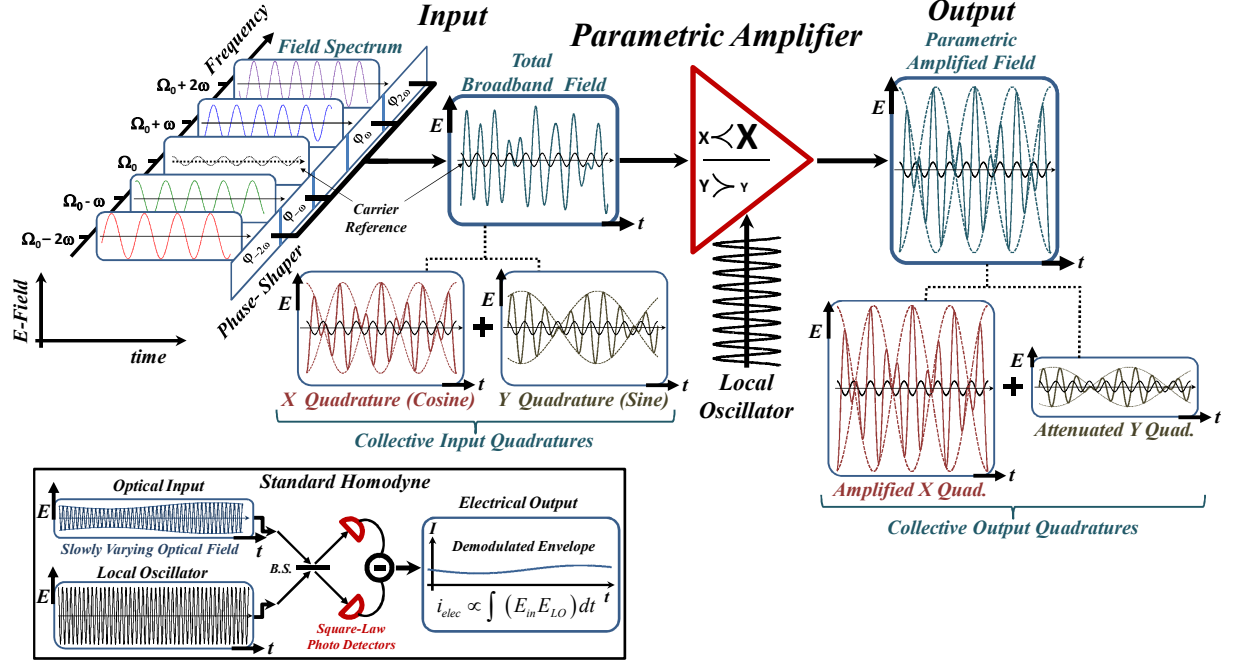


FIG. 1: (color online) **The Parametric Homodyne Process:** In our homodyne method we use an optical parametric amplifier to amplify one quadrature of the broadband optical signal and attenuate the other. The parametric amplifier distinguishes between the two quadratures by the phase of an external local-oscillator, which is the pump for the parametric amplification. Hence, if the parametric gain is strong enough, the resulting output will be nearly proportional to the specific quadrature that was amplified, directly serving as a homodyne measurement. In the illustration, a broadband optical beam is manipulated using a spectral phase shaper so that the  $\Omega_0 \pm 2\omega$  mode-pair generates a **fast** beat envelope only on the *X* quadrature, and the  $\Omega_0 \pm \omega$  mode-pair generates a **slower** beat envelope only on the *Y* quadrature. The total broadband optical field conceals the quadrature information, however, after the measurement amplifier, the *X* quadrature is amplified and the *Y* quadrature is attenuated, such that the resulting parametric output is almost entirely proportional to the *X* quadrature and the **fast** beat is clearly visible. The small black oscillation plotted on top of the various fields is a cosine local-oscillator reference to identify the *X* and *Y* quadratures. The inset shows the standard Homodyne measurement where the electrical nonlinearity of square-law photo-detectors is used to mix the measured input field and the LO. The electrical output, which is limited to MHz to GHz range, is only capable of following very slow variations of the envelope of the input field occurring over millions of optical cycles.

of MHz to GHz range. The detection is also strongly affected by the detectors quantum efficiency and spectral noise, which lead to equivalent decoherence and additional vacuum noise [12–15].

The time dependent description of the two-mode quadratures in equations 2,4 is thus inconvenient for standard homodyne with broadband light, since it cannot be related directly to measurable quantities. Consequently, the common expression for the two-mode quadratures relies on equation 5, using the individual quadratures of the signal and idler modes,  $X_{s,i}, Y_{s,i}$  relative to two correlated LOs at their respective frequencies  $\omega_s, \omega_i$ . Thus, to measure two-mode quadratures and squeezing, the standard procedure requires two homodyne measurements of the independent quadratures of both the signal and the idler using a pair of phase-correlated LOs, followed by low-noise subtraction/summation circuitry [15, 26].

Standard two-mode homodyne however, cannot provide a complete measurement of  $x(\omega)$  in a single shot. Since standard homodyne is a destructive measurement, observation of  $\text{Re}x(\omega) = X_s + X_i$  requires a standard homodyne measurement of both frequency modes, which inevitably destroys the quantum state by photo-detection and prevents consecutive measurement of  $\text{Im}x(\omega) = Y_s - Y_i$ . Splitting the state into two measurement channels is also impossible since splitting introduces additional vacuum noise. Thus, although  $\text{Re}x(\omega)$  and  $\text{Im}x(\omega)$  commute, standard two-mode homodyne can evaluate only one of them in a single shot, which indicates that it can provide the complete quadrature information *only when the phase of the two-mode beat envelope is known and fixed*. For two-mode squeezed vacuum however, which is the major quantum state that is experimentally accessible in two-mode, the envelope phase is random, indicating that standard homodyne can provide only the average fluctuations  $\langle x^\dagger x \rangle = \langle (X_s + X_i)^2 \rangle + \langle (Y_s - Y_i)^2 \rangle$ , but not the single shot value of the quadrature (or its intensity).

With standard two-mode homodyne, each frequency pair of a broadband spectrum requires a homodyne measurement with a separate pair of LOs. In principle however, a single LO should be sufficient to measure the entire spectrum of mode pairs simultaneously, just as all mode pairs of broadband squeezed light can be generated with a single pump laser. To achieve such direct parallel detection over the entire bandwidth, we suggest to exploit a *direct broadband optical nonlinearity* to multiply the fields, instead of the indirect narrowband electronic nonlinearity of photo-detectors.

We present a different approach to the two-mode homodyne (see figure 1), based on

broadband optical parametric amplification, which amplifies one quadrature of the input light and attenuates the other (normally used as the major method to generate squeezed vacuum). With sufficient parametric gain, any given  $X$  quadrature at the input, even if it was originally squeezed, can be amplified above the vacuum noise level and into the "classical regime", which allows *complete freedom in measurement* since quantum vacuum fluctuations are no longer a limiting noise source. Furthermore, if the gain is high enough for the amplified quadrature to dominate the intensity of the output light over the attenuated orthogonal  $Y$  quadrature, measurement of the light intensity at the output will reflect directly a single-shot value of the input quadrature intensity  $x^\dagger x$  (as illustrated in figure 1). Intuitively, the concept of parametric homodyne is easily understood in the limit of large parametric gain, where the quadrature of interest dominates the output light field. However, parametric homodyne method is equally effective in almost any finite parametric gain. Although the output intensity with finite gain does not directly reflect the quadrature intensity, it provides equivalent information about the quadrature, as explained below and in the supplementary information. Specifically, two average intensity measurements, one for each quadrature, allows to uniquely reconstruct both average quadrature intensities.

Notice that the measurement parametric amplifier is not necessarily required to be an ideal squeezer. Specifically, since the attenuated quadrature is not measured, it does not need to be squeezed below vacuum. Consequently, restrictions on the measurement amplifier are considerably relaxed compared to a source of squeezed light, allowing it to operate with much higher gain. The parametric amplification is a *non-demolition* process that provides a *light output*, which allows extraction of the *complete quadrature information*. In the experiment below, we measured the quadrature intensity across a wide spectrum, but in principle, also the quadrature phase could be obtained from the output light. Since the amplified quadrature is nearly insensitive to loss even for moderate gain, it can be split after the parametric amplification to two simultaneous homodyne channels, allowing measurement of both  $\text{Re}[x(\omega)]$  and  $\text{Im}[x(\omega)]$ . The splitting will not hamper the measurement (contrary to standard homodyne), since the added vacuum affects primarily the attenuated quadrature, which is not measured.

It is interesting to examine standard homodyne measurement as a form of parametric amplification. After all, balanced photo-detection produces a down-converted RF field at the difference-frequency between the two optical inputs (LO and signal), similar to optical down-

conversion - the core of parametric amplification. In that view, balanced detection produces photon-electron entanglement, similar to the entangled bi-photons produced by a parametric amplifier; and the well known 'homodyne gain', which enhances the electronic signal above the electronic noise (proportional to the LO amplitude), is analogous to the parametric gain, which enhances the optical quadrature above the vacuum noise. The main differences are that photo-detection destroys the optical fields, whereas the optical nonlinearity preserves them, allowing *non-demolition manipulations*; and that the homodyne gain of the balanced detection is normally high enough to safely neglect the unmeasured quadrature, which cannot be assumed a-priori for the optical case. Clearly therefore, adding a layer of parametric gain before the photo-detection (homodyne or direct intensity), can convert the electronic part of the measurement to be nearly classical, thereby alleviating most of the electronic limitations.

In our experiment, we measured the output spectrum of the parametric amplifier for an input of broadband squeezed vacuum, obtaining the quadrature intensity  $x^\dagger(\omega)x(\omega)$  simultaneously across the entire bandwidth. Although such a measurement of the spectral intensity loses the quadrature phase (or the sign of the real/imaginary parts), it is still highly useful, since it provides sufficient information to measure any quantum state whose quadrature probability distribution is symmetric, which is relevant to a large set of important quantum states, such as Fock-states, squeezed vacuum and symmetric Schrödinger cat-states. For broadband squeezed vacuum, where the envelope phase is of no interest (random), this measurement is ideal.

Mathematically, our method relies on the similarity between the quadrature operators of interest from equation 4  $x = a_s + a_i^\dagger$ ,  $-iy^\dagger = a_s - a_i^\dagger$  and the field amplitude operators at the output of a parametric amplifier,

$$a_s(g) = C(g)a_s + D(g)a_i^\dagger, \quad (6)$$

where  $C$  and  $D$  are the parametric gain coefficients that fulfil  $|C|^2 - |D|^2 = 1$ , and  $g$  is the squeezing gain set by the efficiency of the nonlinear process (the common form is  $a_s(g) = a_s \cosh g + a_i^\dagger e^{i\varphi} \sinh g$ ,  $C = \cosh g$  and  $D = e^{i\varphi} \sinh g$ ). When  $g$  is large, both  $|C|, |D| \approx e^g$ , and the annihilation operator at the amplified output becomes  $a_s(g) \xrightarrow{g \rightarrow \infty} x e^g$  or  $a_s(g) \xrightarrow{g \rightarrow \infty} y^\dagger e^g$ , depending on the pump phase. Although the field operator converges to the quadrature only in the limit of high gain, its relation to the quadrature operators is unique and informative at any finite gain, allowing reconstruction of the quadratures. The significance

of the field-quadrature relation for finite gain is described in the supplementary information.

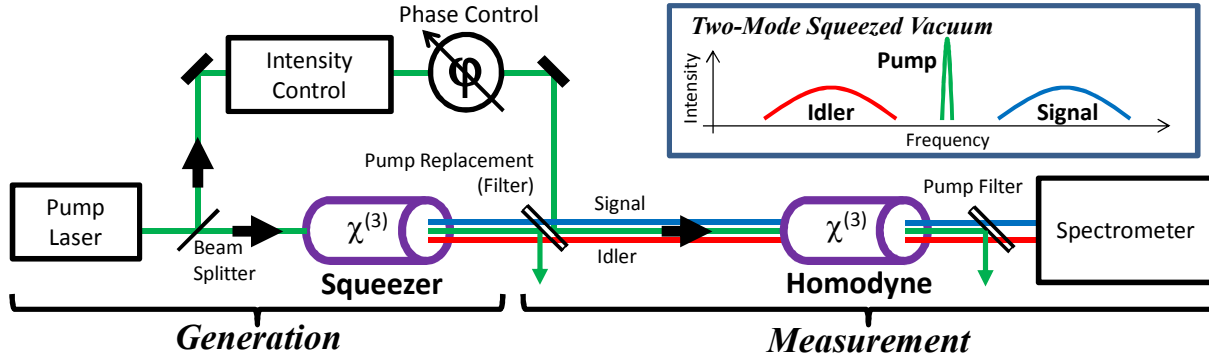


FIG. 2: (color online) **Experimental Concept of the Parametric Homodyne:** (a) Setup - The experiment consists of two parts: 1. generation of broadband squeezed light and then 2. homodyne measurement of the generated squeezing. Broadband two-mode squeezed light is generated via spontaneous four-wave mixing (FWM) in a photonic crystal fiber (PCF) pumped by 12ps laser pulses (786nm). After generation, the pump is replaced by a narrow-band filter to allow independent intensity and phase control, to tune the parametric gain and to select the specific quadrature to be measured. Then the new pump and the FWM enter the second PCF for the homodyne measurement. After the 2nd (measurement) amplifier the pump is separated by a narrow-band filter from the FWM field which is measured by a spectrometer.

Before dwelling into the experimental measurement of broadband squeezing, let us elaborate on the importance of broadband squeezed vacuum [2, 21, 22] as a resource for quantum information, and on the potential to exploit broadband squeezing detection for highly parallel quantum processing. Specifically, a very large bandwidth of symmetrically separated frequency pairs can be generated simultaneously from a single parametric amplifier with a single narrowband pump laser, which can potentially serve as parallel quantum modes (Q-modes) in a quantum processing application [11]. The squeezing bandwidth of a parametric amplifier is limited only by its phase matching and can easily extend over a full optical octave, either by chirped polling of the non-linear medium [23], or by matching of the pump frequency to the zero-dispersion of the medium [24, 25]. Assuming a squeezing bandwidth of 10-100THz (common), the number of simultaneous mode-pairs can easily exceed  $10^5$ .

Two examples can illuminate the great potential of broad bandwidth in quantum information on one hand, and the difficulty of standard methods to exploit it on the other. A



most promising realization for scalable quantum information is to exploit the bandwidth of entangled Q-modes of a quantum frequency comb that is generated by a single parametric oscillator [11, 16]. This approach demonstrated to date the largest entangled clusters of Q-modes and a complete set of quantum gate operations. The limiting factor of this realization is the homodyne measurement bandwidth, where each Q-mode required a precise homodyne measurement using a pair of phase-correlated LOs. A broad bandwidth of Q-modes would require a dense set of correlated LOs and multiple homodyne measurements, quickly multiplying the complexity towards impracticality. Another example is in quantum communication and QKD, where enhanced bandwidth was pursued as an avenue to increase the data rate by increasing the number of bits per photon. Here, the concept is to divide the photon readout time, which is limited by photo-detectors, into multiple short time-bins, which act as an additional time stamp for each photon (or pair) [18, 19]. The time stamp (bin), which is usually detected using a Franson interferometer [27], enhances the number of bits per photon to  $\log_2 N$ , where  $N$  is the number of time-bins. Theoretically, if the bandwidth limit of the detector could be lifted, all time (or frequency) bins could be detected independently, and a much higher flux of photons could be used ( $N$  times higher). This would allow full parallelization of the communication across the available bandwidth and enhancement of the total throughput by factor  $N$  (compared to  $\log_2 N$ ).

Here we exploit for the parametric homodyne measurement the same non-linearity and the same pump that were used to generate the squeezed state in the first place, thus guaranteeing a bandwidth match between the homodyne measurement and the input squeezing. The quadrature information over many frequency pairs is obtained simultaneously by measuring the spectrum of the light at the output of the parametric amplifier, which would allow extreme parallel processing. Since each individual mode-pair is measured independently with just a single LO - the pump, the number of accessible Q-modes (or Q-bits) that could be utilized simultaneously would be multiplied by  $N$  (the number of modes) rather than  $\log_2 N$ .

The experimental concept to demonstrate broadband parametric homodyne (see figure 2), consists of two parts: First, generation of broadband squeezed vacuum, and second, parametric homodyne detection of the generated squeezing. We generate broadband squeezed vacuum by collinear four-wave mixing (FWM) in a photonic crystal fiber (PCF) that is pumped by narrowband picosecond pulses. To measure the generated squeezing, we couple

the generated FWM together with the pump to another PCF which acts as a measurement amplifier (in the experiment this was the same PCF in the backward direction). After the second (measurement) pass we record the parametric output spectrum to extract the quadrature information (shown in figure 3 (a)). Since squeezed vacuum is a gaussian state, its quadrature distribution is completely defined by the second moment. We therefore measure the average spectral intensity (with averaging times of a few 10s of milliseconds) and reconstruct the average quadrature fluctuations  $\langle x^\dagger x \rangle, \langle y^\dagger y \rangle$  (measurement of the intensity distribution is possible with shorter integration time, but not necessary for squeezed vacuum). Already the raw output spectrum demonstrates reduction of the parametric output *below the vacuum noise-level* (defined as the parametric output when the input is blocked) across the entire 55THz, directly indicating broadband squeezing. To verify this, we varied the quadrature squeezing by varying the loss of the input FWM field before the measurement (second) pass through the PCF. As the loss is increased, the squeezing slowly vanishes, and even though the total power entering the fiber diminished, the minimum fringes at the output of the measurement amplifier rose towards the vacuum input level, as shown in the inset of figure 3 (a). More details of the experimental apparatus can be found in the supplementary information.

Due to chromatic dispersion in the filters and windows used in the experiment, the accumulated phase between the FWM and the pump varied across the spectrum, indicating that for some frequencies the stretched quadrature is amplified (bright fringes) while for others the squeezed quadrature is amplified (relatively dark fringes). The specific quadrature to be amplified could be controlled by varying the pump phase.

The extraction of the quadrature information from the measured parametric output assumes knowledge of the parametric gain of the measurement amplifier, which requires calibration of the parametric amplifier. The calibration is a simple process, achieved by recording the output spectrum for a set of known inputs (figure 3 (b)), when blocking various fields (signal, idler or pump). For example: The vacuum level of the parametric amplifier is observed when both the signal and the idler input fields are blocked ( $I_{zsi}$  - zero signal idler). Also, the average number of photons at the input is given by the ratio between the measured output with blocked signal (idler only,  $I_{zs}$  - zero signal) and the vacuum input level  $\langle N_i \rangle = \frac{I_{zs}}{I_{zsi}} - 1$ . This calibration process is fully described in the supplementary information. The parametric homodyne results in figure 3 (c) show  $\sim 1.5$ dB squeezing across the entire

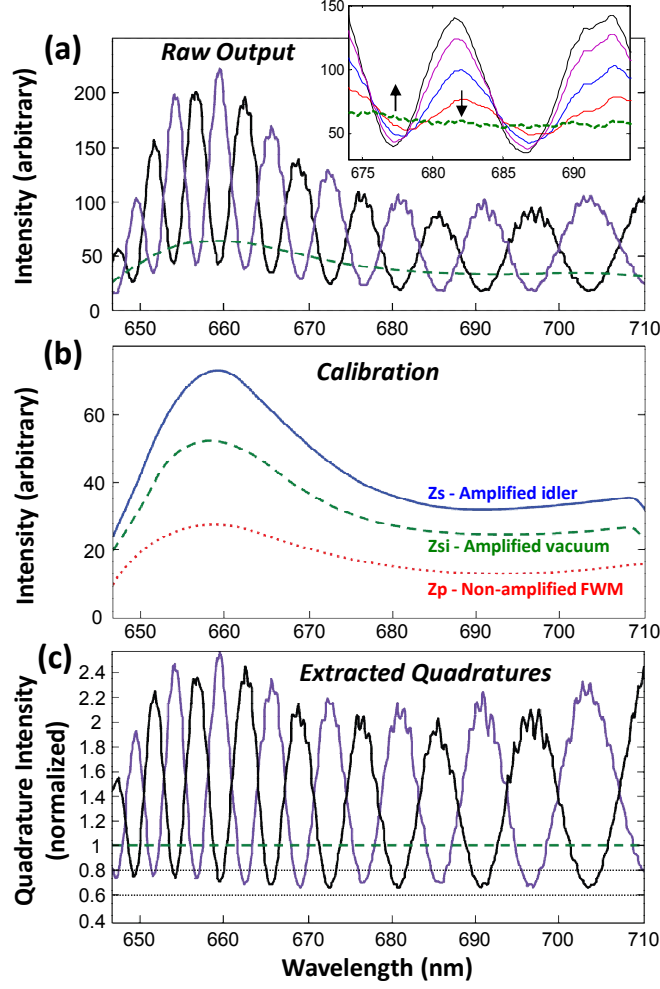


FIG. 3: (color online) **The Parametric Homodyne Measurement Process** includes three stages - raw output measurement (a), calibration (b) and quadrature extraction (c). **(a)** Raw Output Measurements - In the most general case of arbitrary parametric gain, two measurements are needed to extract the quadrature information: 1. amplifying one quadrature (black); and 2. amplifying the other quadrature (purple). The specific quadrature to be amplified is defined by tuning the pump phase. The reduction of the raw output beneath the vacuum-input level (dashed green) directly indicates squeezing. The **inset** shows the effect of loss on the FWM light. As loss is increased, the squeezing is reduced and the observed local minima rise towards the vacuum level (vertical arrows) even though the total input intensity is considerably decreased (a non-classical signature). **(b)** Calibration - To calibrate the parametric amplifier, the output response is measured for a set of three known inputs: 1. idler-input only (blocked signal,  $I_{zs}$  - solid blue), 2. vacuum-input (blocked entire FWM,  $I_{zsi}$  - dashed green), and 3. zero amplification (blocked pump,  $I_{zp}$  - dotted red). **(c)** Extracted Quadratures - With the analysis detailed in the supplementary information, quadrature information is extracted. Quadrature squeezing is evident across the entire 55THz spectrum down to  $\langle x^\dagger x \rangle \approx 0.68$ , 32% below the vacuum level ( $\sim 1.5dB$ ).

55THz bandwidth. To obtain a homodyne measurement across such a large bandwidth with standard homodyne detection would be practically impossible.

The observed squeezing in our experiment is far from ideal, primarily due to use of a pulsed pump, which induces an undesirable time dependence of the parametric gain and phase (via self-phase and cross-phase modulation - SPM and XPM) in the squeezing process, as well as in the parametric homodyne measurement. Since our pulses are relatively long, their time dependence can be regarded as adiabatic, indicating that the instantaneous squeezing (source) and the parametric amplification (measurement) are ideal, but the quadrature axis, squeezing level and gain of each one vary with time (not necessarily at the same rate). Thus, our spectral measurements, which represent a temporal average of the light intensity over the entire pulse, somewhat dim the "expected" squeezing. However, even with a pulsed pump, the various homodyne and calibration measurements are consistent and unequivocal for weak enough pump intensity (see further elaboration regarding the effects of pulse averaging in the supplementary information). With a pure CW pump, as is generally used in squeezing applications, this pulse averaging limitation would not exist. Another limitation of our measurements is the need to re-couple the FWM back into the PCF, which introduces an inevitable loss of 30% and reduces the observed squeezing. This "known" loss can either be avoided completely in other experimental configurations or be easily calibrated out to obtain a worst-case "bare" squeezing level of the measured light source (see supplementary information).

We verified the properties of the parametric homodyne in several ways, which are shown in figures 5 and 6 in the supplementary information. We measured the squeezed quadrature  $\langle x^\dagger x \rangle$ , and the uncertainty area,  $\langle x^\dagger x \rangle \times \langle y^\dagger y \rangle$  of the squeezed state. Ideally, the generated squeezed light should be a minimum uncertainty state of  $\langle x^\dagger x \rangle \times \langle y^\dagger y \rangle = 1$ , independent of the generation gain; and the average intensity of the squeezed quadrature should exponentially decrease with the gain. The results, presented in figure 5 (a-b) of the supplementary information, show a clear reduction of the normalized squeezed quadrature intensity down to  $\langle x^\dagger x \rangle \approx 0.68$  (32% below the vacuum level), and the uncertainty area remains nearly ideal at  $\langle x^\dagger x \rangle \times \langle y^\dagger y \rangle < 1.3$ , up to a pump power of 60mW. Further increase of the pump does not improve the measured squeezing due to pulse effects, and the minimum uncertainty property deteriorated. Based on the measured squeezing, the instantaneous squeezed quadrature at the peak of the pulse was estimated to be better than 3dB (see supplementary informa-

tion). Additional verification measurements of the homodyne process are presented in the supplementary information and in figures 5 (c-d) and 6 in the supplementary information.

Previously, the effect of two parametric amplifiers in series was explored in the context of quantum interference [28]. In such a series configuration, interference occurs between two possibilities for generating bi-photons, either in the first amplifier or in the second, depending on the pump phase. The interference contrast can reach unity when the parametric gain of the two amplifiers is *identical* (assuming no loss), which testifies to the quantum nature of the light in both the single-photon regime [25] and at high-power [24, 28]. Here however, we consider the second amplifier as a measurement device, independent of the source of light to be measured. The source of light can be, but is certainly not limited to be, a squeezing parametric amplifier. Clearly, any other source of quantum light is relevant when homodyne measurement is of interest, such as single photons, Fock states, NOON states, Schrödinger cat states, etc.

A different optical measurement of quantum light was recently reported in [29], where vacuum fluctuations of THz radiation were observed *in time*. There too, an optical nonlinearity (of several THz bandwidth) was utilized for a direct measurement, where the large bandwidth of the nonlinearity was key to enable time sampling of the vacuum fluctuations, well within a single optical-cycle of the measured THz mode.

To conclude, we presented a new approach to optical homodyne measurement with practically unlimited bandwidth, which is based on optical parametric amplification and enables simultaneous quadrature measurement across an unlimited spectrum of two-mode light using a single LO. This measurement removes a major limitation of optical homodyne and opens a wide window for efficient utilization of the bandwidth resource for parallel quantum information processing. An interesting expansion of this concept would be where the pump itself includes more than one mode, for measurement of "hyper" entanglement between different frequency pairs of the frequency comb with a multi-mode pump [11, 30].

This research was funded by the 'Bikura' (FIRST) program of the Israel science foundation (ISF grant #44/14).

---

\* Electronic address: avi.peer@biu.ac.il

[1] A. I. Lvovsky and M. G. Raymer, "Continuous-variable optical quantum-state tomography,"

- Reviews of Modern Physics*, vol. 81, no. 1, p. 299, 2009.
- [2] M. O. Scully and M. S. Zubairy, *Quantum optics*. Cambridge university press, 1997.
  - [3] G. Breitenbach, S. Schiller, J. Mlynek, *et al.*, “Measurement of the quantum states of squeezed light,” *Nature*, vol. 387, no. 6632, pp. 471–475, 1997.
  - [4] D. Smithey, M. Beck, M. G. Raymer, and A. Faridani, “Measurement of the wigner distribution and the density matrix of a light mode using optical homodyne tomography: Application to squeezed states and the vacuum,” *Physical review letters*, vol. 70, no. 9, p. 1244, 1993.
  - [5] A. Ourjoumtsev, R. Tualle-Brouiri, and P. Grangier, “Quantum homodyne tomography of a two-photon fock state,” *Phys. Rev. Lett.*, vol. 96, p. 213601, Jun 2006.
  - [6] A. Ourjoumtsev, H. Jeong, R. Tualle-Brouiri, and P. Grangier, “Generation of optical schrödinger cats from photon number states,” *Nature*, vol. 448, no. 7155, pp. 784–786, 2007.
  - [7] T. C. Ralph and P. K. Lam, “Teleportation with bright squeezed light,” *Phys. Rev. Lett.*, vol. 81, pp. 5668–5671, Dec 1998.
  - [8] A. Furusawa, J. L. Sørensen, S. L. Braunstein, C. A. Fuchs, H. J. Kimble, and E. S. Polzik, “Unconditional quantum teleportation,” *Science*, vol. 282, no. 5389, pp. 706–709, 1998.
  - [9] N. Lee, H. Benichi, Y. Takeno, S. Takeda, J. Webb, E. Huntington, and A. Furusawa, “Teleportation of nonclassical wave packets of light,” *Science*, vol. 332, no. 6027, pp. 330–333, 2011.
  - [10] S. L. Braunstein and P. Van Loock, “Quantum information with continuous variables,” *Reviews of Modern Physics*, vol. 77, no. 2, p. 513, 2005.
  - [11] M. Pysher, Y. Miwa, R. Shahrokhshahi, R. Bloomer, and O. Pfister, “Parallel generation of quadripartite cluster entanglement in the optical frequency comb,” *Physical review letters*, vol. 107, no. 3, p. 030505, 2011.
  - [12] D. Huang, D. Lin, C. Wang, W. Liu, S. Fang, J. Peng, P. Huang, and G. Zeng, “Continuous-variable quantum key distribution with 1 mbps secure key rate,” *Optics express*, vol. 23, no. 13, pp. 17511–17519, 2015.
  - [13] J. Appel, D. Hoffman, E. Figueroa, and A. Lvovsky, “Electronic noise in optical homodyne tomography,” *Physical Review A*, vol. 75, no. 3, p. 035802, 2007.
  - [14] R. Okubo, M. Hirano, Y. Zhang, and T. Hirano, “Pulse-resolved measurement of quadrature phase amplitudes of squeezed pulse trains at a repetition rate of 76 mhz,” *Optics letters*, vol. 33, no. 13, pp. 1458–1460, 2008.
  - [15] A. M. Marino, C. Stroud Jr, V. Wong, R. S. Bennink, R. W. Boyd, *et al.*, “Bichromatic

- local oscillator for detection of two-mode squeezed states of light,” *JOSA B*, vol. 24, no. 2, pp. 335–339, 2007.
- [16] N. C. Menicucci, S. T. Flammia, and O. Pfister, “One-way quantum computing in the optical frequency comb,” *Physical review letters*, vol. 101, no. 13, p. 130501, 2008.
- [17] H. J. Briegel, D. E. Browne, W. Dür, R. Raussendorf, and M. Van den Nest, “Measurement-based quantum computation,” *Nature Physics*, vol. 5, no. 1, pp. 19–26, 2009.
- [18] T. Zhong, H. Zhou, R. D. Horansky, C. Lee, V. B. Verma, A. E. Lita, A. Restelli, J. C. Bienfang, R. P. Mirin, T. Gerrits, *et al.*, “Photon-efficient quantum key distribution using time–energy entanglement with high-dimensional encoding,” *New Journal of Physics*, vol. 17, no. 2, p. 022002, 2015.
- [19] I. Ali-Khan, C. J. Broadbent, and J. C. Howell, “Large-alphabet quantum key distribution using energy-time entangled bipartite states,” *Physical review letters*, vol. 98, no. 6, p. 060503, 2007.
- [20] C. M. Caves and B. L. Schumaker, “New formalism for two-photon quantum optics. i. quadrature phases and squeezed states,” *Physical Review A*, vol. 31, no. 5, p. 3068, 1985.
- [21] L. Davidovich, “Sub-poissonian processes in quantum optics,” *Reviews of Modern Physics*, vol. 68, no. 1, p. 127, 1996.
- [22] R. Loudon and P. L. Knight, “Squeezed light,” *Journal of modern optics*, vol. 34, no. 6-7, pp. 709–759, 1987.
- [23] S. Harris, “Chirp and compress: toward single-cycle biphotons,” *Physical review letters*, vol. 98, no. 6, p. 063602, 2007.
- [24] Y. Shaked, R. Pomerantz, R. Z. Vered, and A. Pe’er, “Observing the nonclassical nature of ultra-broadband bi-photons at ultrafast speed,” *New Journal of Physics*, vol. 16, no. 5, p. 053012, 2014.
- [25] R. Z. Vered, Y. Shaked, Y. Ben-Or, M. Rosenbluh, and A. Pe’er, “Classical-to-quantum transition with broadband four-wave mixing,” *Physical review letters*, vol. 114, no. 6, p. 063902, 2015.
- [26] V. Boyer, A. M. Marino, R. C. Pooser, and P. D. Lett, “Entangled images from four-wave mixing,” *Science*, vol. 321, no. 5888, pp. 544–547, 2008.
- [27] J. D. Franson, “Bell inequality for position and time,” *Physical Review Letters*, vol. 62, no. 19, p. 2205, 1989.

- [28] M. Chekhova and Z. Ou, “Nonlinear interferometers in quantum optics,” *Advances in Optics and Photonics*, vol. 8, no. 1, pp. 104–155, 2016.
- [29] C. Riek, D. V. Seletskiy, A. S. Moskalenko, J. F. Schmidt, P. Krauspe, S. Eckart, S. Eggert, G. Burkard, and A. Leitenstorfer, “Direct sampling of electric-field vacuum fluctuations,” *Science*, vol. 350, no. 6259, pp. 420–423, 2015.
- [30] R. Schmeissner, J. Roslund, C. Fabre, and N. Treps, “Spectral noise correlations of an ultrafast frequency comb,” *Physical review letters*, vol. 113, no. 26, p. 263906, 2014.



## SUPPLEMENTARY INFORMATION

### Single-Mode vs Two-Mode Quadratures in the Homodyne Measurement

While the single mode state is defined by only two quadratures  $(X, Y)$ , yielding a 2D Wigner map, the two-mode state has 4 degrees of freedom  $(X_s, Y_s, X_i, Y_i$  or linear combinations), yielding a 4D Wigner map. For a single mode, standard homodyne can extract the full quadrature in a single shot, allowing complete Wigner reconstruction, whereas two-mode homodyne (standard or parametric) only partially measures the two-mode quadrature in a single shot, setting some limitations on the Wigner reconstruction for two-modes, but not completely preventing it.

A two-mode oscillation requires two phases, conveniently defined as the carrier phase  $((\varphi_s + \varphi_i)/2$  the sum of mode phases) and the beat envelope phase  $((\varphi_s - \varphi_i)/2$  the difference). The quadratures relate only to the carrier phase (cosine or sine), and must therefore carry the envelope phase as an additional degree of freedom. To measure the complete two-mode quadrature in a single shot, the complex value of  $x(\omega) = a_s + a_i^\dagger$  should be obtained [1, 2], both real and imaginary parts:

$$\begin{aligned}
 x_\omega(t) &= x(\omega)e^{-i\omega t} + x^\dagger(\omega)e^{i\omega t} \\
 &= (x + x^\dagger) \cos \omega t + i(x - x^\dagger) \sin \omega t \\
 \text{Re}[x(\omega)] &= x + x^\dagger = X_s + X_i \\
 \text{Im}[x(\omega)] &= i(x - x^\dagger) = Y_s - Y_i.
 \end{aligned} \tag{7}$$

Despite the mathematical similarity of  $\text{Re}x(\omega) = x + x^\dagger$  and  $\text{Im}x(\omega) = i(x - x^\dagger)$  to the definition of the single-mode quadratures  $X = a + a^\dagger, Y = i(a - a^\dagger)$ , their physical meaning is inherently different. The field operators  $a, a^\dagger$  do not commute  $([a, a^\dagger] = 1)$ , whereas  $x, x^\dagger$  do  $([x, x^\dagger] = 0)$ , indicating that the real and imaginary parts of  $x$  can, in principle, be measured simultaneously in a single shot (as opposed to  $x, y$ ).

Thus, since the phase of the envelope relates to commuting observables (as opposed to the carrier phase), it does not reflect a nonclassical property of the quantum light field, but rather defines the temporal mode in which the field is measured. Specifically, the temporal mode of measurement is the beat pattern of frequency  $\omega$ , where the temporal offset of the beat is defined by the envelope phase. This offset, along with other mode parameters, such as polarization, spatial mode, carrier frequency, etc. define the mode of the local oscillator.

Of course, quantum entanglement of the state between the two envelope modes (cosine or sine) is possible, just like entanglement of a single photon (or photon pair, or cat state) between polarization modes, which is widely used for quantum information. However, this quantumness is additional and different, on top of the intra-mode quantum state, which is described by the quadratures.

Since standard homodyne is a destructive measurement, it can measure either  $\text{Re}[x(\omega)]$  or  $\text{Im}[x(\omega)]$  in a single shot. In analogy to light polarization, standard homodyne acts as an absorptive polarizer that detects one polarization but absorbs the other. Parametric homodyne (with only intensity detection) measures the quadrature intensity  $x^\dagger x$ , but not its phase. Since the instantaneous quadrature intensity  $x^\dagger x$  can be evaluated in every shot, not just its mean value, the entire distribution of the intensity can be measured, including higher moments ( $\langle x^\dagger x \rangle, \langle (x^\dagger x)^2 \rangle, \dots$ ).

### Parametric Homodyne with Low Parametric Gain

The quadrature intensity is directly measured by parametric homodyne only in the limit of large gain. However, since two light intensity measurements along orthogonal axes uniquely infer the two quadrature intensities at any finite gain, the information content of a single detection of the output intensity is equivalent to that of the quadrature intensity at any gain. To derive this equivalence, let us examine the relation between the field operators at the output and the quadratures of the input:

$$\begin{aligned} a_s(\theta, g) &= a_s e^{-i\theta} \cosh(g) + a_i^\dagger e^{i\theta} \sinh(g) \\ &= x_\theta e^g + i y_\theta^\dagger e^{-g}, \end{aligned} \tag{8}$$

where  $g$  is the parametric gain and  $\theta$  is the angle of the rotated quadrature axis  $x_\theta = a_s e^{-i\theta} + a_i^\dagger e^{i\theta} = x \cos \theta + y^\dagger \sin \theta$ . As mentioned, the field operator converges in the limit of large gain to an amplified single quadrature operator  $a_s(\theta, g) \rightarrow e^g x_\theta$ , but, this convergence can never be exact since the commutation relation of field operators  $[a, a^\dagger] = 1$  is inherently different than that of quadrature operators  $[x, x^\dagger] = 0$ . To illuminate the smooth transition from a field operator to a quadrature, let us express the field operator for any finite parametric gain in the form of a generalized quadrature operator along an axis of a complex angle  $\vartheta = \theta + i\gamma$ ,

$$a_s(g) = M(\tilde{x} \cos \vartheta + \tilde{y}^\dagger \sin \vartheta = M\tilde{x}_\vartheta, \tag{9}$$

where the imaginary part of the quadrature axis and the normalization factor  $M$  relate to the gain  $g$  by  $\tanh \gamma = e^{-2g}$ ,  $M^2 = 2 / \sinh 2\gamma$ .

Thus, the single-shot measurement of the output light intensity with any parametric gain reflects the intensity of the "generalized" quadrature at this gain value, and not the standard (real) quadrature. The commutation relation of these generalized quadratures is

$$[\tilde{x}_\vartheta, \tilde{x}_\vartheta^\dagger] = 1/M^2 \approx e^{-2g}, \quad (10)$$

where the approximation is valid already for moderate gain of  $g \geq 1$ . Consequently, the commutator of the measured generalized quadratures, converges very quickly to that of the real quadratures.

### Quantum Derivation of the Parametric Amplified Output Intensity

To model quantum mechanically the parametric homodyne process, we derive an expression for the parametric output intensity (photon-number) operator of the signal (or idler) mode,  $N_s(g) = a_s^\dagger(g)a_s(g)$  ( $g$  is the squeezing parameter set by the efficiency of the nonlinear process) in terms of the input complex quadratures  $x, y$ .

The output field operator of any parametric amplifier can be expressed as  $a_s(g) = Ca_s + Da_i^\dagger$  (equation 6), where the coefficients  $C$  and  $D$  are generally complex. Since field operators must fulfil  $[a_s^\dagger(g), a_s(g)] = 1$ , the two coefficients  $C$  and  $D$  must obey  $|C|^2 - |D|^2 = 1$ , which leads to the common description of  $C = \cosh g$  and  $D = e^{i\varphi} \sinh g$ . However, the attributed phase of the parametric process, which is determined by the pump phase and the phase matching conditions in the non-linear medium, can also be expressed explicitly, leaving the two coefficients  $C, D$  real and positive (rather than complex), using  $a_s(g, \theta) = (Ca_s e^{i\theta} + Da_i^\dagger e^{-i\theta})e^{i\theta_0}$ . Since the overall phase  $\theta_0$  does not affect the photon-number calculations, we may discard it as  $\theta_0 = 0$ . In this expression we account for the phase of the pump as a rotation of the input quadrature axis -  $a_{s,i} \rightarrow a_{s,i}(\theta) = a_{s,i} e^{i\theta}$ . Accordingly, the rotated complex quadrature operators (equation 4) become  $x_\theta = a_s e^{i\theta} + a_i^\dagger e^{-i\theta}$  and  $y_\theta = -i(a_i e^{i\theta} - a_s^\dagger e^{-i\theta})$ .

Parametric amplification directly amplifies one input quadrature and attenuates the other, as evident by expressing the field operators  $a_s(g)$  at the amplifier output using the

quadrature operators  $x, y$  of the input:

$$\begin{aligned} a_s(g, \theta) &= \frac{C+D}{2}x_\theta + i\frac{C-D}{2}y_\theta^\dagger \\ &= e^g x_\theta + e^{-g} y_\theta^\dagger. \end{aligned} \quad (11)$$

Finally, the parametric photon-number operator at the output becomes:

$$\begin{aligned} N_s(g, \theta) &= a_s^\dagger(g, \theta)a_s(g, \theta) = -\frac{1}{2}(N_i - N_s + 1) + \\ &\quad + \frac{1}{4}(C+D)^2 x_\theta^\dagger x_\theta + \frac{1}{4}(C-D)^2 y_\theta^\dagger y_\theta \\ &= -\frac{1}{2}(N_i - N_s + 1) + \frac{1}{4}e^{2g} x_\theta^\dagger x_\theta + \frac{1}{4}e^{-2g} y_\theta^\dagger y_\theta. \end{aligned} \quad (12)$$

The first term  $-\frac{1}{2}(N_i - N_s + 1)$  does not depend on the pump phase and contributes only an offset to the expectation value. Typically, this offset is approximately  $-\frac{1}{2}$  since the signal and idler photon numbers are usually identical in the absence of loss. The remaining two terms are essential to the measurement since they are proportional to the *two-mode quadrature intensities*. The second term  $\frac{1}{4}(C+D)^2 x_\theta^\dagger x_\theta = \frac{1}{4}e^{2g} x_\theta^\dagger x_\theta$  accounts for the amplification of one quadrature, and the third term  $\frac{1}{4}(C-D)^2 y_\theta^\dagger y_\theta = \frac{1}{4}e^{-2g} y_\theta^\dagger y_\theta$  accounts for the attenuation of the other. If the measurement gain considerably exceeds the generation gain, such that  $e^{2g} x_\theta^\dagger x_\theta \gg e^{-2g} y_\theta^\dagger y_\theta$  the quadrature intensity can be directly extracted (after calibration) from a single measurement. When the measurement gain is not large enough and the attenuated quadrature cannot be neglected, the two quadrature intensities can be easily extracted using a pair of measurements; setting the pump phase to amplify one quadrature ( $\theta=0$ ) and then to amplify the other ( $\theta=\pi/2$ ), as illustrated in figure 3.

### Calibration of the Parametric Amplifier

To obtain the quadrature information from the measured output intensity, the parametric amplifier must be calibrated. The required parameters are the gain coefficients  $|C|$  and  $|D|$  which are linked by  $|C|^2 - |D|^2 = 1$  (without the phases, which define the quadrature axis), the average photon-numbers of the two input modes  $\bar{N}_s, \bar{N}_i$  (to evaluate the offset term  $(-\frac{1}{2}(\bar{N}_i - \bar{N}_s + 1))$ ), and the overall detector response per single photon  $n_0^2$ . Thus, independent measurements of the four parameters,  $|C|$  or  $|D|$ ,  $\bar{N}_s$ ,  $\bar{N}_i$  and  $n_0^2$ , is required. In most squeezing applications however, the offset term may be treated as just  $-\frac{1}{2}$ , since it is proportional to the photon-number difference, which is generally zero for squeezed light when the loss is nearly symmetric.

Using equation 6, the measurement output (proportional to the FWM intensity) is

$$I_s = n_0^2 [|C|^2 \bar{N}_s + |D|^2 (\bar{N}_i + 1) + C^* D \langle a_s^\dagger a_i \rangle + C D^* \langle a_s a_i^\dagger \rangle]. \quad (13)$$

For calibration we use measurements that are independent of phase-coherent terms ( $\langle a_s^\dagger a_i \rangle = \langle a_s a_i^\dagger \rangle = 0$  or  $D=0$ ), allowing us to write  $I_s = n_0^2 [|C|^2 \bar{N}_s + |D|^2 (\bar{N}_i + 1)]$ .

We first measure the output intensity in two scenarios: 1.  $I_{zsi}$ , blocking the signal and idler (vacuum input) and 2.  $I_{zs}$ , blocking the signal (only idler input)<sup>1</sup>. These measurements provide (with the aid of equation 13)  $I_{zsi} = n_0^2 |D|^2$  and  $I_{zs} = n_0^2 |D|^2 (\bar{N}_i + 1)$ , indicating that the ratio between these two measurements provides the idler average photon-number  $\bar{N}_i = I_{zs}/I_{zsi} - 1$ . Note that these two measurements act as a simple method for acquiring the input number of photons independent of the parametric gain. A measurement of the signal photon-number  $\bar{N}_s$  can be easily acquired by measuring the output idler intensities in the same way.

Next, we use the knowledge of the input photon-numbers for calibrating the overall detector response  $n_0^2$ . We measure: 3.  $\tilde{I}_{zp}$ , blocking the pump (zero amplification,  $|C| = 1, |D| = 0$ , letting the signal and idler through). Again, from equation 13 we find  $n_0^2 = I_{zp}/N_s$ .

Once the detector response is obtained, we can obtain the parametric gain coefficients  $|C|, |D|$  with the  $I_{zsi}$  measurement, since  $|D|^2 = I_{zsi}/n_0^2$  (and  $|C|^2 = |D|^2 + 1$ ).

The calibration process is needed only once for any measured input, as long as the parametric measurement gain is constant, and as long as the average photon-number difference  $\bar{N}_i - \bar{N}_s$  does not change (typically for squeezed input, this difference is simply zero).

### Quadrature Extraction (Avergae)

The two quadratures cannot be measured simultaneously, but their average intensities can both be extracted from two measurements of the parametric output intensity, amplifying

---

<sup>1</sup> In analogy to the engineering formalism for evaluating linear systems by measuring their response in various cases, termed: zero input response (ZIR) and zero state response (ZSR), we use a similar index for the various parametric responses: zero signal (ZS), zero idler (ZI), zero signal and idler (ZSI) and zero pump (ZP)

one quadrature first ( $I_X$ ) and then the other ( $I_Y$ ), according to

$$\begin{aligned}\langle x^\dagger x \rangle &= \frac{1}{r^2 - q^2} [r(I_X/n_0^2 - p) - q(I_Y/n_0^2 - p)] \\ \langle y^\dagger y \rangle &= \frac{1}{r^2 - q^2} [r(I_Y/n_0^2 - p) - q(I_X/n_0^2 - p)],\end{aligned}\tag{14}$$

where  $n_0^2$  is the detector response per single photon and the coefficients  $p, q, r$  are:

$$\begin{aligned}p &= \frac{1}{2}(\bar{N}_s - \bar{N}_i - 1) \\ q &= \frac{1}{4}(|C| + |D|)^2 \\ r &= \frac{1}{4}(|C| - |D|)^2.\end{aligned}\tag{15}$$

## Experimental Setup

In our experiment (figure 4 shows a more detailed configuration), we generate an ultra broadband two-mode squeezed vacuum via collinear four-wave mixing (FWM) in a photonic-crystal fiber (PCF), that is pumped by narrowband 12ps pulses at 786nm with up to 100mW average power. The broad bandwidth is obtained by closely matching the pump wavelength to the zero-dispersion of the fiber at 784nm [25], resulting in a signal and idler bandwidth of  $\sim 55$ THz each, with  $\sim 90$ THz mean frequency separation between the mode centers (700nm - signal center, and 900nm - idler center). After generation, the pump is separated from the FWM field into a different optical path by a narrowband filter (NBF1 - Semrock NF03-808E-25), allowing independent control of the relative pump phase. The pump phase is actively locked to the phase of the FWM using an electro-optic modulator and a fast feedback loop. Both the FWM and pump fields are reflected back (mirrors M1, M2) towards the PCF for a second pass, which then acts as the homodyne measurement. The final parametric amplified spectrum (after the second "homodyne" pass) is filtered from the pump (NBF2 - Semrock NF03-785E-25) and measured with a cooled CCD-spectrograph (SpectraPro 2300i).

In order to partially compensate for the temporal pulse effects due to SPM of the pulsed pump, we used the original pump pulse from the first pass through the PCF also for the second pass. This guaranteed that the pump and the FWM accumulated nearly the same phase modulation (either SPM for the pump or XPM for the FWM light). Polarization manipulations were used to tune the effective parametric gain in the second (measurement) pass independently of the squeezing strength in the first pass: Since the phase matching conditions in the PCF are polarization dependent, the observed FWM spectrum is generated only by one polarization of the pump (this fact was extensively verified). Thus, rotating the

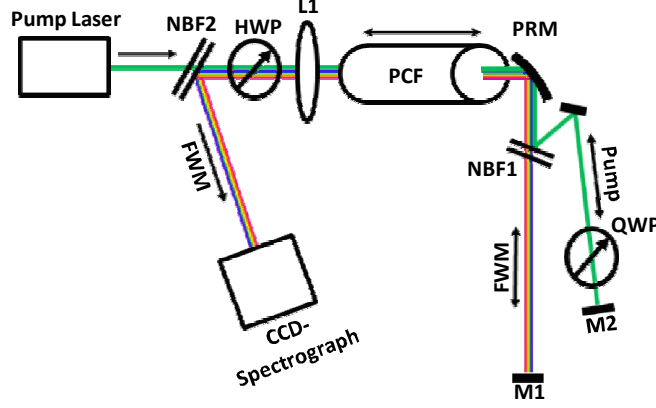


FIG. 4: (color online) **Experimental Setup of the Parametric Homodyne** The experiment consisted of two parts: 1. generation of broadband squeezed light (propagating from left to right) and then 2. homodyne measurement of the generated squeezing (propagating back from right to left). Broadband two-mode squeezed light is generated via spontaneous four-wave mixing (FWM) in a photonic crystal fiber (PCF) pumped by 12ps laser pulses ( $786\text{nm}$ ) (collimated at the output with a parabolic mirror PRM). After generation, the pump and the FWM are separated into two paths by a narrow-band filter (NBF1) allowing the pump phase and polarization to be tuned independently. Both pump and FWM are reflected back by folding mirrors (M1, M2) for a second pass through the PCF, now acting as a measuring device. The specific FWM quadrature to be amplified is selected by tuning the pump phase, and the amplification gain is controlled by manipulation of the pump polarization using the half and quarter wave plates (HWP, QWP) before the fiber and after it. After the 2nd (measurement) pass through the PCF the FWM field is separated from the pump by a narrow-band filter (NBF2) and directed towards a CCD-spectrograph, where the amplified spectrum is measured.

pump polarization before the first pass with a half wave plate (HWP) we could transfer part of the pump power through the fiber without affecting the FWM. This power could later be used in the 2nd pass by rotating its polarization back to the PCF axis with a quarter wave plate (QWP) in the pump beam path. This extra pump power accumulated almost the same phase modulation as the FWM, but without affecting the squeezing generation.

The various calibration measurements were performed by manipulating the FWM light between the passes either by physically blocking the FWM beam (vacuum input) or pump beam (zero amplification) or with a high efficiency optical long-pass filter (idler input

only) (Semrock FF776-Dio1). The two orthogonal homodyne measurements (amplifying the squeezed quadrature or the stretched quadrature) were acquired by tuning the offset of the active feedback loop that locked the pump phase.

### Effects of the Pulsed Pump

In our experiment the pump for both generation of the squeezed light and for the parametric homodyne measurement (2nd pass), is a pulsed laser of  $\approx 12\text{ps}$  duration (a more detailed experimental configuration is shown in figure 4). Since the bandwidth of the generated FWM (55THz) is much larger than the pump bandwidth ( $< 0.1\text{THz}$ ) we could account for the main affect of the pulse shape as an adiabatic variation of the parametric gain and phase modulation (SPM, XPM) along the temporal profile of the pump pulse. Thus, the adiabatic variation can be discretized in time, referring to time instances within a single pulse as separate parametric events of varying gain and phase. However, since the integration time of the photodetectors in the CCD-spectrograph is much longer ( $\sim 10\text{ms}$ ), the measured homodyne data is averaged over the entire shape of many pulses.

The effect of the pulse on the parametric gain alone changes the generated squeezing and the measurement gain with time, measuring weak squeezing with weak parametric gain at the edges of the pulse, and strong squeezing with strong parametric gain at the peak. The phase modulation (SPM,XPM) of the FWM process has a more severe effect, since it modulates *in time* the quadrature axis to be amplified. As a result, due to the pump pulse shape, the amplified quadrature axis of the FWM field rotates with time. Luckily, when the pump itself experiences nearly the same phase modulation (SPM) it can still act as a near perfect LO (phase regarding) for measuring the FWM, even after passage through the fiber. The small residual difference between the pump SPM and the FWM XPM causes the amplified FWM quadrature to rotate with time, mixing different quadrature axes together in the same measurement, smearing out some of the squeezing.

Ideally, we would like to extract the maximum squeezing that occurs at the peak of the pulse from the time averaged measurements. To estimate this peak squeezing we numerically simulated the entire FWM generation and parametric amplification along the pump pulse with 50fs temporal resolution (corresponding to the coherence time of the FWM). The simulation incorporated the measured pump pulse energy, the measured loss and fiber



coupling efficiencies, and an assumed hyperbolic-secant temporal shape of the pump pulse (12ps). Using the simulation we could calculate both the average and the peak outputs of the process, allowing us to estimate the squeezing at the peak of the pulse from the measured averaged homodyne output. Figure 6 (in the supplementary information) demonstrates the relation between the peak homodyne output and the average homodyne output, as the parametric measurement gain is varied. As long as the generation pump power does not exceed a specific limit ( $\sim 60\text{mW}$  in our experiment), the pulse averaging only affects the absolute measured squeezing values (which can be roughly estimated) but not the expected trends of the experiment (increasing the loss, the squeezing power or the parametric power).

### Expanded Results

To verify the properties of the parametric homodyne, we measured the quadrature squeezing  $\langle x^\dagger x \rangle$ , and the uncertainty area,  $\langle x^\dagger x \rangle \times \langle y^\dagger y \rangle$  of the squeezed state as described in the main text.

Another important verification of our squeezing measurement is to observe the effect of loss on the measured quadrature squeezing and stretching. We measured the quadrature intensities after applying a set of known attenuations (30%–66% loss), and reconstructed the 'bare' quadratures before loss, which indeed collapsed to the same value, as shown in figure 5 (c,d) (in the supplementary information).

The effect of loss on the quadrature intensity can be regarded as propagation through a beam-splitter with one open port. The relations between the operators of the two inputs ( $a_1, a_2$ ) and two outputs ( $b_3, b_4$ ) of the beam-splitter can be defined as  $b_3 = Ta_1 + Ra_2$  and  $b_4 = Ta_1 - Ra_2$ , where  $T$  and  $R$  are the transmission and reflection (loss) amplitudes. In these terms, the quadrature operator at output port 3 is:  $X_3 = TX_1 + RX_2$ , and the expectation value of the quadrature intensity is

$$\langle X_3^2 \rangle = |T|^2 \langle X_1^2 \rangle + |R|^2 \langle X_2^2 \rangle + 2RT \langle X_1 \rangle \langle X_2 \rangle. \quad (16)$$

Assuming a vacuum state at the open input port 2, the final expression becomes;

$$\langle X_3^2 \rangle = |t|^2 \langle X_1^2 \rangle + |r|^2. \quad (17)$$

Hence, the 'bare' quadratures, before the loss, can be reconstructed using

$$\langle x^\dagger x_{bare} \rangle = (\langle x^\dagger x_{measured} \rangle - |r|^2) / |t|^2. \quad (18)$$

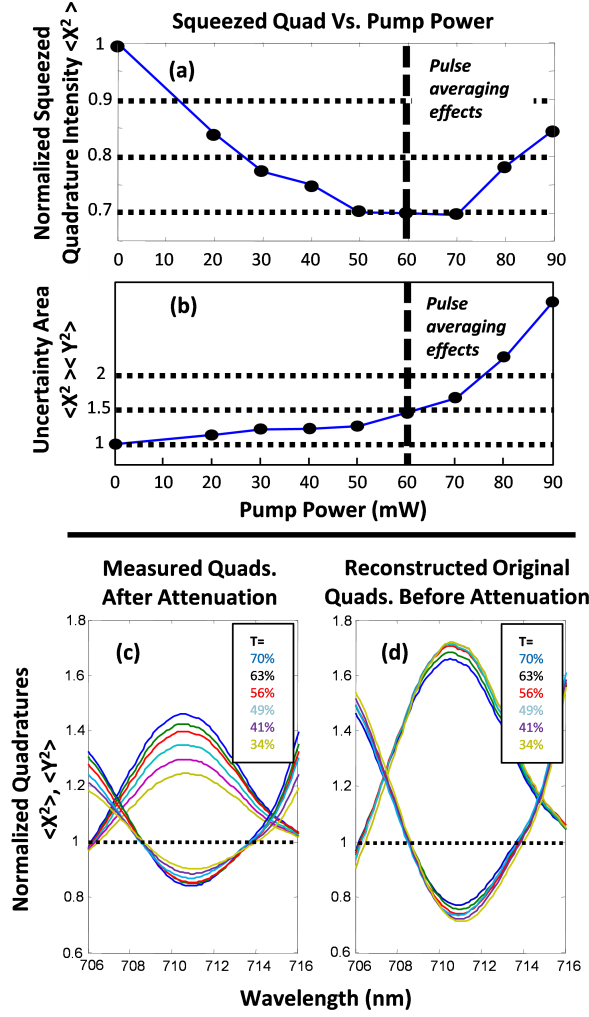


FIG. 5: **Expanded Homodyne Results:** (a) Measured Squeezed Quadrature as a Function of Squeezing Strength ( $696nm$ ) - (solid line for guidance only). As the squeezing strength in the first pass is increased, the measured squeezed quadrature decreases down to  $\langle x^\dagger x \rangle \sim 0.68$  at a pump power of  $\sim 60mW$ . Further increase of the pump degrades the observed squeezing due to temporal effects of the pulsed pump. (b) Minimum Uncertainty Conservation ( $696nm$ ) - (solid line for guidance only). Ideal squeezed vacuum is a minimum uncertainty state of  $\langle x^\dagger x \rangle \langle y^\dagger y \rangle = 1$ , independently of the squeezing strength. Up to a pump power of  $60mW$ , the uncertainty area is indeed nearly conserved ( $\langle x^\dagger x \rangle \langle y^\dagger y \rangle < 1.3$ ). Beyond this limit the pulse-averaging effect washes out the minimum uncertainty property. (c),(d) (color online) The Effect of Loss on the Squeezed State - (c). We apply a series of loss values (30% to 66%) to a given squeezed state and observe the influence on the squeezed/stretched quadratures. (d) shows the reconstructed "bare" squeezed/stetched quadratures that calibrated-out the loss from all the curves of (c), demonstrating collapse of all the curves to nearly the same value, as expected.

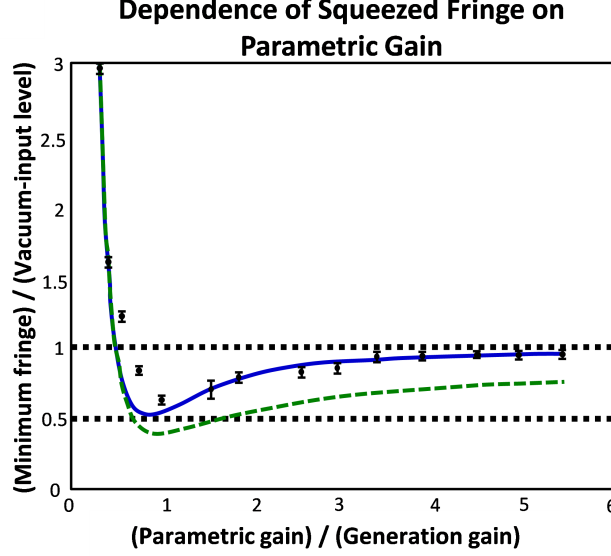


FIG. 6: (color online) **Convergence of the Relative Output (compared to the vacuum level) for High Measurement Parametric Gain (654nm):** When the parametric gain is large enough, the squeezed quadrature can be directly obtained from the relative output - the ratio between the output with input and the output with vacuum (blocked) input. For increased measurement gain (but constant input squeezing) the relative parametric output should therefore converge to a constant level, directly indicating the absolute quadrature intensity. To observe this, we varied the pump intensity in the 2nd (measurement) pass up to 5.5 times the intensity used for generating the broadband squeezing in the 1st (generation) pass. This convergence of the relative output (dots) ( $(\text{Measurement gain}) \setminus (\text{Generation gain}) > 3$ ) approached a constant level of  $\sim 5\%$  below the vacuum level. When the measurement gain is reduced, the relative output decreases due to a quantum interference effect, reaching maximum visibility when the squeezing generation gain is equal to the measurement gain ( $(\text{Measurement gain}) \setminus (\text{Generation gain}) = 1$ ). In this regime, the general measurement becomes indirect (although the squeezing effect is still directly evident), and a pair of measurements (amplifying one quadrature and then the other) is needed for extracting the quadrature information. Below the level of identical gain, the observed output strongly rises over the vacuum level, obscuring the direct evidence of squeezing; however, the quadrature information can still be extracted (though with reduced accuracy) using the same pair of measurements. The solid (blue) curve indicates a numerical simulation of the relative output, assuming the measured pump pulse energy and FWM loss, and an estimated nonlinear coefficient, fiber coupling efficiency and hyperbolic-secant pulse shape. For comparison, we included the simulated result for the relative output at the peak of the pulse (dashed green).

As a complementary evaluation, we studied the parametric measurement-amplifier output as a function of its own gain, while maintaining the squeezing generation gain constant. For this, we gradually increased the pump power in the second pass up to 5.5 times the pump power that generated the squeezing in the first pass. When the parametric gain is strong enough, the output intensity relative to the vacuum level (without input) is directly proportional to the input quadrature. Hence, we expect the relative-output to stabilize as the parametric gain is increased, and indeed the observed reduction below the vacuum level stabilized at 5%. Figure 6 (in the supplementary information) shows the measured results and addresses the pulse effects on this measurement.

---

\* Electronic address: avi.peer@biu.ac.il

- [1] E. Huntington, G. Milford, C. Robilliard, T. Ralph, O. Glöckl, U. L. Andersen, S. Lorenz, and G. Leuchs, “Demonstration of the spatial separation of the entangled quantum sidebands of an optical field,” *Physical Review A*, vol. 71, no. 4, p. 041802, 2005.
- [2] F. A. Barbosa, A. S. Coelho, K. N. Cassemiro, P. Nussenzveig, C. Fabre, M. Martinelli, and A. S. Villar, “Beyond spectral homodyne detection: complete quantum measurement of spectral modes of light,” *Physical review letters*, vol. 111, no. 20, p. 200402, 2013.